

Proc. of the XXVII Intern. School on Physics of Semiconducting Compounds, Jaszowiec 1998

## CdSe LAYERS OF BELOW CRITICAL THICKNESS IN ZnSe MATRIX: INTRINSIC MORPHOLOGY AND DEFECT FORMATION

I. SEDOVA, T. SHUBINA, S. SOROKIN, A. SITNIKOVA, A. TOROPOV, S. IVANOV

Ioffe Physical-Technical Institute, Russian Academy of Sciences  
194021 St. Petersburg, Russia

AND M. WILLANDER

University of Gothenburg/Chalmers University, 412 96 Gothenburg, Sweden

Three main stages of the intrinsic morphology transformation of MBE grown CdSe fractional monolayers in ZnSe with increase in their nominal thickness  $w$  in the 0.1–3.0 monolayer range were found using both structural and optical characterization techniques. Emergence of the extended (15–30 nm) CdSe-enriched quantum-dot-like pseudomorphic islands at  $w > 0.7$  monolayer with the density increasing up to  $2.5 \times 10^{10} \text{ cm}^{-2}$  at  $w = 2.8$  monolayer is clearly displayed in the optical properties of CdSe fractional monolayer nanostructures. The below critical thickness CdSe fractional monolayers having extremely high quantum efficiency can be very perspective as an active region of ZnSe-based blue-green lasers.

PACS numbers: 78.45.+h

### 1. Introduction

The interest in a CdSe/ZnSe heteropair, significantly increased during last several years, is dictated by two reasons. First, the CdSe/ZnSe heterostructures can produce a light emission within the 460–530 nm spectral range and are characterized by a high luminescence efficiency, which makes them very perspective as a new active region of the light-emitting devices. Secondly, the CdSe/ZnSe heteropair is very similar to the well studied InAs/GaAs system employed for investigation of self-organizing quantum dots (QDs) [1], although it is more difficult to obtain the 3D quantum confinement in the (Zn,Cd)Se nanostructures because of the much smaller exciton Bohr radius ( $r_B$ ) ( $\approx 3$  nm). Epitaxial growth of CdSe on ZnSe meets with a number of problems. One of them is the formation of extended defects as a result of stress relaxation, when the CdSe nominal thickness ( $w$ ) exceeds the critical one, which in turn results in a dramatic decrease in a photoluminescence (PL) intensity [2]. Using optical measurements, transmission

electron microscopy (TEM) and estimating the CdSe thickness by the reflection high-energy electron diffraction oscillation technique, it was determined that the CdSe critical thickness ( $t_{cr}$ ) on ZnSe is around 3 monolayers (MLs) [2, 3].

By varying the molecular beam epitaxial (MBE) growth conditions and thickness of thin CdSe layer on a ZnSe surface, three different regimes have been reported: (i) Stranski–Krastanov (SK) island growth mode (above  $t_{cr}$ ) [4–6], including thermal activation regime [7], (ii) pseudomorphic growth of thin CdSe or ZnCdSe quantum-well-like (QW-like) layers (below  $t_{cr}$ ) [8–10], and (iii) coexistence of extended islands and the alloy-like phase ( $w \leq 1$  ML) [11–13]. The SK growth mode was found to produce the dot-like CdSe-based islands with lateral sizes far beyond 10 nm, which cannot provide sufficient 3D confinement. Moreover, it has also been shown that reliable SK growth mode can be realized on the atomically flat buffer layer, e.g. on a GaAs surface cleaved in ultrahigh vacuum [6]. The pseudomorphically grown CdSe/ZnSe heterostructures ( $w < 3$  ML) are characterized by a decrease in a PL peak line width with the reduction of  $w$ , observed even in a sub-monolayer region, which contradicts an expectable line width increase for thin QWs due to potential fluctuation on interface roughness. Zhu et al. [8] have interpreted this fact for sub-monolayer  $w$  region by the formation of uniform ZnCdSe alloy layer at the CdSe/ZnSe interface. The recent investigations have revealed the complicated structure of fractional monolayers (FMs) involving both the alloy-like homogeneous layer, which can probably be formed by small, with respect to  $r_B$ , islands, and extended 2D ones [11–13].

In this paper we present results of systematic structural (plan-view TEM) and optical (PL and PL excitation (PLE)) studies of CdSe/ZnSe FM structures with  $w = 0.1$ – $3.0$  ML range, grown by both conventional MBE and migration enhanced epitaxy (MEE). Transformation of the intrinsic morphology of CdSe layer, observed on the TEM images, as a function of  $w$  is well consistent with the PL spectra behavior, demonstrating also reasonable agreement with previously reported data.

## 2. Experiment

The structures were grown pseudomorphically to GaAs (100) substrates at a temperature of 280°C. The samples contain a 50–80 nm ZnSe buffer layer and a 10 nm ZnSe cap layer with the single CdSe FM sandwiched in between. The nominal thickness of CdSe FM for both MBE and MEE techniques varies in the  $w = 0.1$ – $3.0$  ML range. The ZnSe layers were grown in the MBE mode under the VI/II  $\approx 1 : 1$  growth condition at a growth rate  $\approx 100$  Å/min. The CdSe growth rate in the MBE mode (27 Å/min) is calibrated using the value obtained in MBE growth of semibulk ZnCdSe layers grown at the VI/II  $\approx 1 : 1$  flux ratio and taking account of the experimentally established dependence of a Cd incorporation coefficient on the Se/Cd flux ratio [14]. In contrast to the MBE growth mode, FM structures grown in the MEE mode demonstrate a more than threefold reduced CdSe growth rate. The details of the CdSe FM growth by MBE and MEE have been reported elsewhere [11]. The PL measurements were performed at low (1.8 K) temperature using the 351 nm line from a cw Ar<sup>+</sup> laser. Tungsten lamp emission dispersed by a single-grating monochromator is used for PLE measurements. The

plan-view samples for TEM study using Philips EM420 electron microscope were prepared by chemical polishing in two different solutions.

### 3. Results and discussion

Figure 1 shows the experimental relationship between  $w$  and the energy position of PL maximum for the whole set of samples grown in MBE and MEE modes along with the data available in the literature. The dotted lines are guide for the eye. For both types of the structures the peak energy decreases gradually with the increase in  $w$ , which agrees well with the published data [3, 9, 15]. The

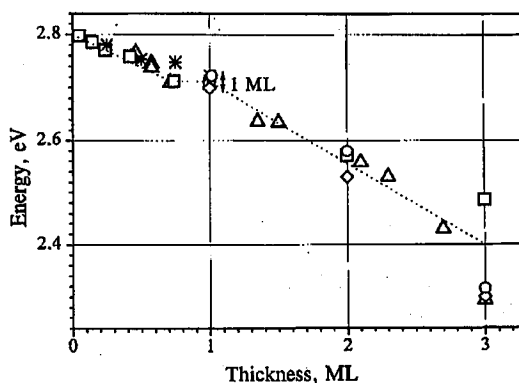


Fig. 1. Experimental dependence of PL peak energy position on the CdSe FM nominal thickness  $w$  for MBE (open triangles) and MEE (open squares) grown samples. Stars, open circles, and diamonds present the data adopted from Refs. [9, 3, 15], respectively.

two regions with different slopes may be distinguished in this curve with some indication of the plateau in the 0.6–1 ML thickness range. The samples of both groups (MBE and MEE), each being grown under the same specific conditions, give the close PL peak energies at the same  $w$ . This PL energy vs.  $w$  behavior more likely reflects the intrinsic morphology transformation process. In the first region, with  $w < 0.5$ –0.6 ML, the CdSe FM can be considered as a uniform array of small CdSe islands, with sizes smaller than  $r_B$ . Since excitons cannot be efficiently localized on these islands, the system may be treated as a ZnCdSe alloy-like layer. Rather steep variation of PL peak energy between 0.5–0.6 ML seems to be due to an appearance of relatively large 1 ML high islands with sizes exceeding  $r_B$ . The next region of  $w$  ( $w = 0.6$ –1 ML) is characterized by nearly constant energy position of the PL maximum lying within the range admissible for 1 ML thick CdSe QW (2.71–2.73 meV). Further increase in the amount of deposited material results in the essential red shift of the PL maximum, accompanied by larger dispersion of the experimental points, which is probably related to the thickness and size fluctuations of CdSe-enriched dot-like islands.

These speculations can be confirmed by the complementing results of plan-view TEM and PL studies presented in Fig. 2. A narrow single peak (full width at half maximum (FWHM) is of  $\approx 5$ –8 meV) is observed at  $w < 0.5$  ML. Such PL

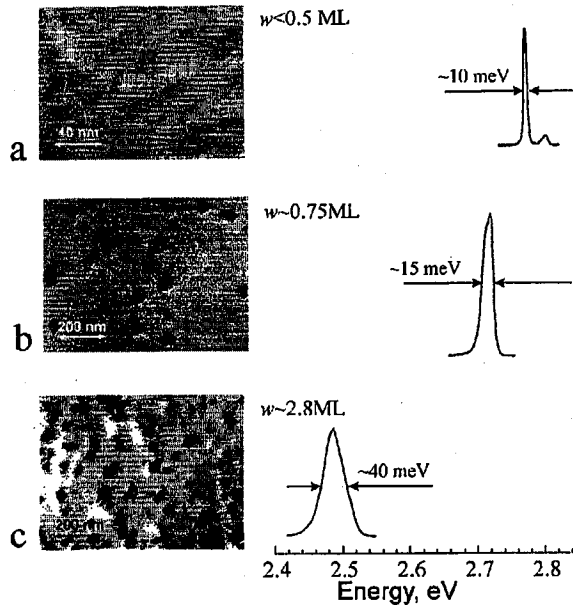


Fig. 2. Plan-view TEM images and relative PL spectra of single CdSe FMs in ZnSe matrix with different nominal thickness:  $< 0.5$  ML (a),  $0.75$  ML (b),  $\approx 2.8$  ML (c).

spectrum is typical of alloy-like flat QWs. As a rule, no extended objects have been observed in the respective TEM images, at least larger than  $10$  nm in diameter (Fig. 2a). However, more careful examination of the  $0.5$  ML samples under the different reflection conditions allowed us to discover extremely small self-organized objects related to the CdSe FM and not observed in the cap ZnSe layer (will be published elsewhere [16]). Although their lateral size is comparable with our TEM resolution ( $\approx 20$  Å), a comparative analysis of TEM images obtained on MBE and MEE samples enables one to conclude that MEE grown CdSe FMs are characterized by smaller dispersion of nano-object sizes with the pronounced maximum at  $\approx 25$  Å. In the MBE case, the size dispersion of CdSe islands is larger, whereas the mean island size is smaller than in MEE samples. These observations indicate different mechanisms of Cd incorporation for the two growth modes, with the MEE mode being more equilibrium one.

The increase in  $w$  within the  $0.5$ – $1$  ML range results in the appearance in TEM image of the extended CdSe-based islands with the lateral sizes of  $15$ – $40$  nm and a density of  $(4$ – $5) \times 10^9$   $\text{cm}^{-2}$  (Fig. 2b). The islands with the lateral size exceeding  $\approx 30$  nm seem to be relaxed with formation of equally-orientated borderland defects. In the relative PL spectrum, this is accompanied by an appearance of doublet peaks with the  $13$ – $17$  meV total FWHM and the  $5$ – $8$  meV FWHM of the high energy component, which indicates a coexistence of two different (alloy- and island-like) phases [11]. This observation is valid for both MBE and MEE structures, though the PL line width is systematically smaller for the MEE samples.

At  $w > 1$  ML, but below the critical one, the density of the CdSe-enriched self-organized dot-like islands dramatically increases up to  $(2-3) \times 10^{10} \text{ cm}^{-2}$  keeping the island sizes in the 15–40 nm range (Fig. 2c). The density of the largest relaxed islands practically does not vary, being of about 10% of the total island density, while other 90% of islands (15–30 nm) seem to be pseudomorphic. Some islands reveal well-resolved square shape with the equally oriented facets. No structural defects are observed out of the large CdSe-based islands. The PL intensity increases dramatically, becoming about 350 times stronger in the 2.8 ML FM with respect to 0.25 ML one. Simultaneously, the PL band becomes rather broad and non-homogeneous (PLE data see below) in accordance with observable CdSe FM morphology.

One should stress that the permanent error introduced in the phase-contrast TEM image by the ZnSe cap layer having certain thickness can enlarge the real size of the islands, which may be of  $\approx 10$  nm for the smallest islands, but hardly compared with  $\tau_B$ .

The 5 K PL and PLE spectra for two CdSe FM samples with different  $w$  are presented in Fig. 3. For comparison the PLE spectra of reference ZnCdSe QWs with the PL peak energies close to those of the respective FM samples are shown as well. In the vicinity of 1 ML (Fig. 3a), the PLE spectra from FM and QW look similar. Strong exciton resonances are observed in 1.2 FM samples with even smaller electron-hole background than in the reference QW. The FM PLE spectra monitoring from different points of the PL contour, marked by arrows, vary only in intensity, which confirms the homogeneous and QW-like nature of

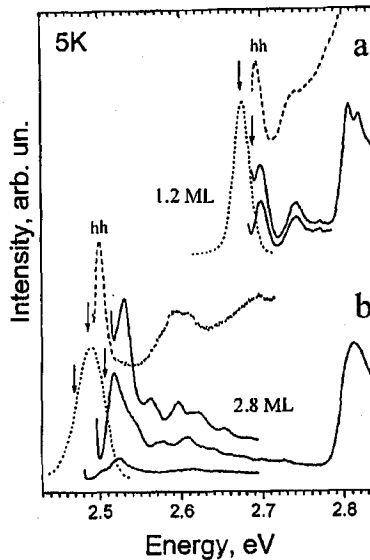


Fig. 3. Low temperature PL (dotted lines) and PLE (solid lines) spectra for two CdSe FM samples with  $w$  of 1.2 ML (a) and 2.8 ML (b). PLE spectra of reference ZnCdSe QWs are shown by dashed lines.

light-emitting objects. The increase in  $w$  up to 2.8 ML results in non-uniform broadening of PL line (Fig. 3b). Contrary to the PLE spectra of the reference QW structure, the spectra of the FM move in step with the registration positions. The well-pronounced series of peaks separated by  $\approx 30$  meV, which is close to the ZnSe LO phonon energy, are observed for the FM structure. This indicates that excitons created in the ZnSe matrix relax to FM insertion through a phonon-assisted mechanism as a whole. The difference between the spectral position of the lowest observed PLE peaks and the related PL maximum increases drastically from  $\approx 20$  meV for 1.2 ML sample to  $\approx 45$  meV for 2.8 ML one, confirming more complex localization potential in the more thicker FM, obviously related to the higher level of structural irregularities.

In summary, it has been shown that the pseudomorphic MBE and MEE growth of CdSe FM on ZnSe results in three different types of CdSe layer morphology in dependence on the quantity of deposited CdSe, starting from alloy-like homogeneous layer ( $w < 0.5$  ML) and finishing with the self-organized dot-like CdSe-based extended islands (15–40 nm in diameter). The obtained results enable one to develop the MBE technological regimes suitable for the fabrication of real CdSe-based QDs.

### Acknowledgment

This work was supported in part by the Russian Foundation for Basic Research and by the Program of Ministry of Science of RF "Physics of Solid-States Nanostructures".

### References

- [1] S. Fafard, D. Leonard, J.L. Merz, P.M. Petroff, *Appl. Phys. Lett.* **65**, 1388 (1994).
- [2] H. Zajicek, P. Juza, E. Abramov, O. Pankratov, H. Sitter, M. Helm, G. Brunthaler, W. Faschinger, K. Lischka, *Appl. Phys. Lett.* **62**, 717 (1993).
- [3] S. Fujita, Yi-hong Wu, Y. Kawakami, Sh. Fujita, *J. Appl. Phys.* **72**, 5233 (1992).
- [4] H.C. Ko, D.C. Park, Y. Kawakami, S. Fujita, Sh. Fujita, *Appl. Phys. Lett.* **70**, 3278 (1997).
- [5] D. Hommel, K. Leonardi, H. Heinke, H. Selke, K. Ohkawa, F. Gindele, U. Woggon, *Phys. Status Solidi B* **202**, 835 (1997).
- [6] S.H. Xin, P.D. Wang, Aie Yin, C. Kim, M. Dobrowolska, J.L. Merz, J.K. Furdyna, *Appl. Phys. Lett.* **69**, 3884 (1996).
- [7] H. Kirmse, R. Schneider, M. Rabe, W. Neumann, F. Henneberger, *Appl. Phys. Lett.* **72**, 1329 (1998).
- [8] S. Yamaguchi, Y. Kawakami, S. Fujita, Sh. Fujita, Y. Yamada, T. Mishina, Y. Masumoto, *Phys. Rev. B* **54**, 17312 (1996).
- [9] Z. Zhu, H. Yoshihara, K. Takebayashi, T. Yao, *Appl. Phys. Lett.* **63**, 1678 (1993).
- [10] U. Neukirch, D. Weckendrup, W. Faschinger, P. Juza, H. Sitter, *J. Cryst. Growth* **138**, 849 (1994).
- [11] S.V. Ivanov, A.A. Toropov, T.V. Shubina, S.V. Sorokin, A.V. Lebedev, I.V. Sedova, P.S. Kop'ev, G.R. Pozina, J.P. Bergman, B. Monemar, *J. Appl. Phys.* **83**, 3168 (1998).

- [12] A.A. Toropov, S.V. Ivanov, T.V. Shubina, A.V. Lebedev, S.V. Sorokin, P.S. Kop'ev, G.R. Pozina, J.P. Bergman, B. Monemar, *J. Cryst. Growth* **184/185**, 293 (1998).
- [13] F. Gindele, C. Markle, U. Woggon, W. Langbein, J.M. Hvam, K. Leonardi, K. Ohkawa, D. Hommel, *J. Cryst. Growth* **184/185**, 306 (1998).
- [14] S. Ivanov, S. Sorokin, I. Krestnikov, N. Faleev, B. Ber, I. Sedova, Yu. Kudryavtsev, P. Kop'ev, *J. Cryst. Growth* **184/185**, 70 (1998).
- [15] S.J. Hwang, W. Shan, J.J. Song, Z.Q. Zhu, T. Yao, *Appl. Phys. Lett.* **64**, 2267 (1994).
- [16] A. Sitnikova, T. Shubina, I. Sedova, S. Sorokin, A. Toropov, S. Ivanov, M. Willander, *Proc. E-MRS, Strasbourg 1998* (to be published in *Thin Solid Films*).